

# Experimental Study of a Fast Gas-Particle Separator

R. Andreux, G. Ferschneider  
Institut Français du Pétrole  
Solaize B.P.3, 69390 Vernaison, France

M. Hémati  
Laboratoire de Génie Chimique  
UMR CNRS 5503, ENSIACET, INPT  
BP 1301, 5 rue Paulin Talabot, 31106 Toulouse Cedex 1, France

O. Simonin  
Institut de Mécanique des Fluides de Toulouse  
UMR CNRS/INPT/UPS 5502  
Allée du Pr. Soula, 31400, Toulouse, France

## **Key words**

Separator, cyclone, FCC, experiment, modelling

## **Abstract**

A horizontal rapid gas-particle separator dedicated to the Fluid Catalytic Cracking process was tested on a small scale cold Circulating Fluidized Bed. Air (density  $1.2 \text{ kg/m}^3$ , dynamic viscosity  $1.8 \times 10^{-5} \text{ Pa.s}$ ) and typical FCC particles (density  $1400 \text{ kg/m}^3$ , mean diameter  $70 \text{ }\mu\text{m}$ ) are used. The inlet gas velocity is kept constant at  $7.3 \text{ m/s}$  while the inlet solid loading and the separator dipleg back pressure range from  $0$  to  $16 \text{ kg/kg}$  and  $100$  to  $500 \text{ Pa}$ , respectively. Solid collection efficiency and pressure drop are studied. A model based on cyclone concepts is proposed. The solid collection efficiency increases with the inlet solid loading and reaches an asymptotic value close to  $95 \%$  when the inlet loading is above  $5 \text{ kg/kg}$ . Two flow regimes are observed in the separator dipleg through the range of inlet solid loadings, related to the available flow section modification and the interstitial gas entrainment. At constant gas collection efficiency, the separator pressure drop is maximum under single-phase flow conditions and reaches a minimum when the inlet solid loading is close to  $2.5$ . The pressure drop increases again for higher inlet solid loading. The final

modeling allows good prediction of the separator operation for all inlet solid loading conditions when the gas collection efficiency is at 100 %.

## **Introduction**

Gas-particle separation at the top of the riser reacting zone is a major issue in the Fluid Catalytic Cracking process which converts large quantities of heavy liquid oils to lighter and more valuable gas products. Indeed, the higher the efficiency and the swiftness of the separation, the lower will be the particle catalyst losses and the gas products post-riser cracking are. Thus, rapid riser termination has become an increasingly important issue over the last fifteen years (Avidan, 1990, Gauthier et al., 2000, Knowlton, 2002). Previously, riser termination devices consisted of simple disengagement systems (Figure 1) located at the riser top leading to rough catalyst and hydrocarbon products separation. Multiple stages of cyclones were needed to collect the amount of entrained catalyst, while hydrocarbons post-riser residence times in the reactor dilute phase were typically 15-45 s which are significantly longer than the required residence time in the riser for the reaction to be completed (typically 1-5 s).

Over the years, separator design improvements and breakthrough have been proposed to increase the collection efficiencies and to reduce the pressure drop and the residence time of the gas phases. Andreux et al. (2005) presented the development of a fast gas-solid separator from lab scale to industrial FCC application which strongly decreases the gas residence time during the separation. The effects of the cyclone geometry and of the phases outlets on the cyclone operation have been extensively reported in the literature (for example : square-shaped cyclone separator by Qiu et al., 1999 and Su and Mao, 2006. Cyclone length by Hoffman et al., 2001. Pneumatic extraction, by Gil et al., 2002).

Theoretically, high efficiency gas-particle separation can easily be reached under the operating conditions of an FCC unit. For example, first-stage cyclones typically reach 99%

collection efficiencies. Nevertheless, the cyclone efficiency could dramatically collapse during transient steps (unit shut down and upset for example) since cyclone flexibility is low, leading to high catalyst losses.

In this context, attractive concepts for new separator developments can logically be based on (i) the separator flexibility across a wide range of operating conditions in terms of inlet gas velocity and solid mass flux (ii) the gas-particle separation swiftness (iii) the relative unimportance of the separation efficiency with respect to the two previous points so long as the particle collection efficiency is always greater than an acceptable value (for example 80 %). Most importantly, pressure drop of such new separators must be low for practical reasons related to the FCC units operation.

In this context, a horizontal short contact gas-particle separator is studied on a small scale cold make-up of an FCC riser.

## **Method and Materials**

### **The cold pilot-scale Circulating Fluidized Bed**

The cold pilot-scale CFB is presented in Figure 2. The riser is 11 m high with a square cross-section of  $11 \times 11$  cm. In order to visualise the gas-solid flow, all is made of transparent altuglass. Humidified air (density  $1.2 \text{ kg/m}^3$ , dynamic viscosity  $1.8 \times 10^{-5} \text{ Pa.s}$ ) is injected at the bottom of the riser through a perforated plate containing 64 holes of 8 mm diameter. Previous experimental studies had shown that electrostatic phenomena disappear for a relative humidity close to 80% (Andreux, 2001). The gas flow rate is measured using a rotameter before injection into the riser. FCC powder (density  $1400 \text{ kg/m}^3$ , mean diameter  $70 \text{ }\mu\text{m}$ ) is injected horizontally through a 100 mm-diameter L-valve ended by a diaphragm with a square cross-section of 2.5 cm. The injection is made 100 mm above the distributor with a horizontal velocity of approximately 2.5 m/s. Both phases are conveyed vertically upward and are

separated at the top of the riser with the rapid riser separator termination and a classic Swift-cyclone. Particles then move downwards through the dipleg of the cyclone into a dense fluidized bed for storage or are diverted into an initially empty fluidized tank for global solid mass flux measurement.

### **The separator**

The horizontal short contact time gas-particle separator is presented in Figure 3. Gas-particle suspension enters the separator vertically upward and is then centrifuged in half-turn elbow. Particles segregate at the external wall of the separator, and then move vertically downward through the solid outlet, the so-called separator dipleg. With a sufficient high back pressure exerted on the separator dipleg outlet, the gas flow reverts upward and exits through the horizontal gas outlet placed in the center of the separator head. Inlet and dipleg sections are square and exactly the same as the riser section while the gas outlet section is cylindrical.

### **Experimental program**

Experiments were carried out at a superficial velocity of 7.3 m/s and solid circulation mass fluxes from 21 to 133 kg/m<sup>2</sup>s. This corresponds to inlet solid loadings ranging between 2 and 15 kg solid/kg air. The back pressure exerted at the outlet of the separator dipleg is modified to make the gas collection efficiency sweep the [60-100] % range. The solid collection efficiency is measured with a graduated column placed at the bottom of the cyclone which collects the residual particles traveling in the gas outlet flow of the separator. The gas collection efficiency is measured thanks to local velocity profile measurements provided by a Pitot tube placed in the monophasic flow of the gas outlet of the cyclone.

## **Results and Analyses**

### **Collection efficiency: effect of the solid/gas mass flux ratio**

The gas and particle collection efficiencies with no back pressure exerted on the separator dipleg are shown in Figure 4. Three regimes are observed through the whole range of the inlet solid loading.

In the first regime with inlet solid loading from 0 to 1, a strong effect of the inlet solid loading is observed. The gas and the particle collection efficiencies increase significantly when the inlet solid loading increases from infinite dilution. A linear dependence of the particle collection efficiency on the solid loading is found. Extrapolation of the solid collection efficiency to infinite dilution leads to a value close to 62 %, which is the same value as the gas collection efficiency measured in the single-phase flow condition. Gas and particle collection efficiencies are equal to 73 % and 85 % when the maximum solid loading of this regime is reached, respectively.

In the second regime with inlet solid loading from 1 to 5, the sensitivity of the solid loading on the particle collection efficiency is divided by a factor of 10 (the maximum value is 94 %) while the gas collection efficiency is constant (73 %).

In the third regime with inlet solid loading from 5 to 15, the particle collection efficiency is constant while the gas collection efficiency decreases significantly to return to the single-phase flow value (62 %).

Visual observations of the flow showed that (i) throughout the first regime, the available flow section in the dipleg decreases when increasing the solid loading (ii) throughout the third regime, the separator dipleg is fully filled with rapid moving downwards particles which entrain the interstitial gas. The trends measured in the first and the third regimes are explained by these two phenomena which compete with themselves in the second regime.

According to the literature on cyclones, a decrease in the solid collection efficiency is generally observed when the inlet solid loading exceeds a value close to 1 kg/kg (Ushiki et al., 1994. Tuzla and Chen, 1992). Such trend is not observed in the present separator.

### **Collection efficiency: effect of the dipleg back pressure**

The gas and the solid collection efficiencies are presented in Figure 5. Increasing the separator dipleg back pressure allows the maximum gas collection efficiency (100 %) to be reached. In contrast, the solid collection efficiency is mildly affected because the particle segregation phenomena along the half-turn elbow mostly rules over the particle re-entrainment irrespective of the gas flow rate. Consequently, it is quite obvious that the gas flow reverts in a very dilute zone of the separator. This zone is far from the near-wall region where most of the particles are. The flow in the half turn elbow is then vertically stratified.

### **Separator pressure drop**

Three global pressure drops are measured through the separator :

- The pressure drop measured between the separator dipleg and the gas outlet,  $\Delta P_{\text{control}}$ . It must be monitored for the separator operation control since it directly impacts the gas separation efficiency.
- The pressure drop measured between the gas/solid inlet and the dipleg. It is not used when controlling the operated separator.
- The pressure drop measured between the gas/solid inlet and the gas outlet of the separator,  $\Delta P_{\text{separator}}$ , called the separator pressure drop. Our study is focusing on this one because it directly impacts on the unit operation.

The separator pressure drop at fixed gas collection efficiency is presented in Figure 6. It is maximum under single-phase flow conditions and reaches a minimum of 150-200 Pa for an inlet loading close to 2.5 kg/kg, irrespective of the gas collection efficiency. It always increases again when further increasing the inlet loading. The trend is reminiscent of the

cyclone studied by Dry et al. (1993), which was characterized by a maximum pressure drop under single-phase conditions, a minimum pressure drop at an inlet loading equal to 0.5, and a subsequent rise when further increasing the inlet loading. Couturier and Stevens (1993) reported a similar increase at high loadings in an industrial CFB. They suggested that the energy necessary to accelerate the solids at the entrance of the cyclone becomes a significant contribution to the overall pressure drop at high loadings. The decrease in the cyclones pressure drop is generally attributed to the gas vortex decaying due to wall friction which increases with the cyclone surface area and the solid loading. According to this concept, the small wall-flow contact area of our separator explains the larger range of inlet loadings for which the decrease in the pressure drop is observed.

## **Discussion and Modeling**

### **Possible separator improvements**

The gas outlet solid loading for all the studied conditions is presented in Figure 7. It is nearly independent upon the back pressure exerted on the separator dipleg, *i.e.* the gas collection efficiency. Consequently, the gas outlet solid loading variations are predominantly a consequence of the inlet solid loading (Figure 8). The independency of the amount of non separated particles upon the gas flow hydrodynamics in the separator is then underlined and the vertically stratified flow structure in the half turn elbow, previously mentioned, is confirmed. Then, given a constant inlet gas velocity, the particle collection efficiency of the separator is more related to geometric concepts than to hydrodynamic concepts. Consequently, further separator improvements can be achieved acting independently on the external side curve radius of the separator to get better solid collection efficiency and on the internal side design to get better gas collection efficiency and lower pressure drop.

## Modeling the separator at 100 % gas collection efficiency

Assuming the solid separation phenomenon in the present separator and in cyclones is quite similar, the inlet solid loading effect can be empirically correlated accordingly to Hoffmann et al. (1991) :

$$\eta_s(c) = \frac{k_1 c^{k_2} + \eta_{s,0}}{k_1 c^{k_2} + 1}$$

where  $k_1$  and  $k_2$  are constants. Fitting  $k_1$  and  $k_2$  ( $k_1=1.17$  and  $k_2=0.52$ ), the experimental results are perfectly predicted through all the range of inlet solid loading (Figure 9).

In a similar way, the pressure drop is modeled following Barth's and Mushchelknautz' proposals for cyclones (1956, 1972, 1980). The total pressure drop is stated as the sum of the separator body and the vortex finder pressure drop contributions,  $\Delta P_{body}$  and  $\Delta P_{outlet}$  respectively :

$$\Delta P_{body} = \frac{1}{2} \rho_g V_{a,outlet}^2 \frac{D_{outlet}}{D_{sep}} \left( \left( \frac{V_{a,outlet}}{V_{t,outlet}} - \frac{W_{sep}}{0.5D_{sep}} f \right)^{-2} - \left( \frac{V_{t,outlet}}{V_{a,outlet}} \right)^2 \right)$$

$$\Delta P_{outlet} = \frac{1}{2} \rho_g V_{a,outlet}^2 \left( \left( \frac{V_{t,outlet}}{V_{a,outlet}} \right)^2 + K \left( \frac{V_{t,outlet}}{V_{a,outlet}} \right)^{4/3} \right)$$

where  $V_{a,outlet}$  is the axial outlet gas velocity,  $D_{outlet}$  the gas outlet diameter,  $D_{sep}$  the separator diameter,  $V_{t,outlet}$  the tangential gas velocity at the entrance of the gas outlet duct,  $W_{sep}$  the width of the separator,  $f$  the friction factor given by the sum of the air and the particle contributions,  $f = f_{air} + f_{particles}$ , with  $f_{air} = 0.005$  for a separator with smooth wall and  $f_{particles} = 0.008 c_{inlet}^{0.5}$ ,  $c_{inlet}$  the inlet loading, and  $K = 4.4$  for vortex finders with sharp edges.

Barth's paper gives the tangential gas velocity,  $V_{t,outlet}$ , as a function of the tangential gas velocity at the separator wall after the flow squeezing in the inlet region,  $V_{t,wall}$ . Adapting the correlation to our geometry leads to :



$$V_{t,outlet} = V_{t,wall} \left( \frac{D_{sep}}{D_{outlet}} \right) \left( 1 + \frac{0.5\pi D_{sep} W_{sep} f V_{t,wall}}{Q_{g,inlet}} \right)^{-1}$$

where  $Q_{g,inlet}$  is the inlet volumetric flow rate, and  $V_{t,wall}$  is related to the inlet gas velocity and the separator dimensions through the ratio of the moment of momenta of the gas inlet and the gas flowing along the wall after the inlet squeezing,  $\alpha = ((D_{sep} - D_{inlet})V_{inlet}) / (D_{sep} V_{t,wall})$ .

Muschelknautz proposed an algebraic correlation for the determination of  $\alpha$  in cyclones. In the present study, tuning  $\alpha$  to fit the measured pressure drop for single phase flow is acceptable since the separator geometry is quite different from the one of a cyclone. We then find  $\alpha = 0.86$ . As the Bath-Muschelknautz model conceptually accounts for the vorticity decay when increasing the inlet loading, it then predicts the decrease in the pressure drop. However, the increase in the pressure drop at high loading can not be predicted by this approach. Assuming that the increasing pressure drop is mainly due to a phenomenon caused by the separated particle flow, the following correlation is proposed :

$$\Delta P_{particle} = K_{particle} \alpha_{particle,outlet} \rho_{particle} V_{a,outlet}^2$$

where  $K_{particle}$  is a constant which is tuned to fit the pressure drop slope at high inlet loading :

$K_{particle} = 2$ ,  $\alpha_{particle,outlet}$  is the volumetric solid concentration in the gas outlet,  $\rho_{particle}$  the solid density.

Both decreasing and increasing in the pressure drop below and above the critical inlet loading are well predicted, as shown in Figure 10. The importance of the introduced contribution in the pressure drop is clearly underlined.

## **Conclusion**

A horizontal rapid gas-particle separator dedicated to the Fluid Catalytic Cracking process was tested on a small scale cold Circulating Fluidized Bed. Its flexibility is studied over a wide range of operating conditions. The inlet gas velocity is kept constant at 7.3 m/s while the

inlet solid loading varies from 0 to 16 kg/kg. The conceptual basis of the separator allows the gas collection efficiency to be modified between 60 % and 100 % modifying the pressure balance between the gas and solid outlets. The effects on the solid collection efficiency and on the pressure drop are studied. A cyclone model from the literature is adapted to the present separator geometry and is improved to account for phenomena that appear at high solid loadings.

For a fixed pressure difference between the gas and solid outlets, the solid collection efficiency increases with the inlet solid loading and reaches an asymptotic value close to 95 % when the inlet loading is above 5 kg/kg. Two flow regimes are observed in the separator dipleg : when increasing the inlet loading (*i*) at low inlet loadings, the available flow section decreases and the gas collection efficiency then increases (*ii*) at high inlet loadings, the interstitial gas entrainment becomes predominant and the gas collection efficiency then decreases.

At constant gas collection efficiency, the separator pressure drop is maximum in single-phase flow condition and reaches a minimum when the inlet solid loading is close to 2.5. The pressure drop then rises again for higher loadings.

Upon adapting a cyclone model to our separator geometry, the decreasing pressure drop for increasing inlet solid loading is well predicted. Accounting for the increasing in the pressure drop at high inlet solid loadings requires an additional term that is related to the amount of entrained particles in the gas outlet stream. The final model gives good prediction of the separator operation in 100 % gas collection efficiency condition.

## **Nomenclature**

$c$	inlet solid loading (kg/kg).
$D_{\text{outlet}}$	diameter of the separator gas outlet (m).

$D_{\text{sept}}$	diameter of the separator (m).
$f$	wall friction factor of the gas-particle suspension.
$k_1$	first constant appearing in the solid collection efficiency correlation.
$k_2$	second constant appearing in the solid collection efficiency correlation.
$K$	constant appearing in the separator outlet pressure drop correlation.
$K_{\text{particle}}$	constant related to the non separated particle contribution in the pressure drop correlation.
$V_{\text{a,outlet}}$	axial outlet gas velocity (m/s).
$V_{\text{inlet}}$	inlet gas velocity (m/s).
$V_{\text{t,outlet}}$	tangential gas velocity at the entrance of the gas outlet duct (m/s).
$V_{\text{t,wall}}$	tangential gas velocity at the separator wall (m/s).
$W_{\text{sep}}$	width of the separator (m).
$\Delta P_{\text{body}}$	pressure drop of the separator body (Pa).
$\Delta P_{\text{outlet}}$	pressure drop of the vortex finder (Pa).
$\Delta P_{\text{particle}}$	pressure drop due to the non separated particles (Pa).
$\alpha$	ratio of the moment of momenta of the gas in the separator.
$\alpha_{\text{particle,outlet}}$	solid volumetric concentration in the gas outlet of the separator ( $\text{m}^3/\text{m}^3$ ).
$\rho_{\text{g}}$	gas density ( $\text{kg}/\text{m}^3$ ).
$\rho_{\text{particle}}$	particle density ( $\text{kg}/\text{m}^3$ ).
$\eta_{\text{s}}$	solid collection efficiency (%).
$\eta_{\text{s},0}$	solid collection efficiency under infinite dilute conditions (%).

## **References**

Andreux, R., 2001, Experimental and numerical study of a gas-solid separator of a cold FCC make-up, *PhD Thesis, Institut National Polytechnique de Toulouse, France.*

Andreux, R., Verstraete, J., Gauthier, T., Roux, R., Ross, J.-L., 2005, An efficient FCC riser separation system : from R&D to industrial practice, in *IFSA – Industrial Fluidization South Africa, Johannesburg, 16-17 Nov. 2005, Proceedings, A. Luckos and P. Smit eds., 2005, pp. 225-244, South Africa Institute of Mining and Metallurgy.*

Avidan A., Owen H., Schipper P., 1990, FCC Closed Cyclone System, *oil Gas J.*, (88): 56-62.

Barth, W., 1956, Berechnung und Auslegung von Zyklonabscheidern au Grund neuerer Untersuchungen (in German), *Brennstoff-Wärme-Kraft*, 1:1-9.

Couturier, M.F., Stevens, D., 1993, Capture efficiency of an industrial CFB cyclone, *4<sup>th</sup> Int. CFB Conference*: 540-544.

R.J. Dry, R.W. White, T. Joyce, 1993, Correlations of solids circulation rate in circulating fluidized bed systems, *4<sup>th</sup> Int. CFB Conference*: 621-627.

Gauthier, T., Bayle, J., Leroy, P, 2002, FCC : Fluidization phenomena and technologies, *Oil & Gas Science and Technology, Revue de l'IFP*, 55(2):187-207.

Gil, A., Cortés, C., Romeo, L.M., Velilla, J., 2002, Gas-particle flow inside cyclone diplegs with pneumatic extraction, *Powder Techn.*, 128(1):79-91.

Hoffmann, A.C., Arends, H., Sie, H., 1991, An experimental investigation elucidating the effect of solid loading on cyclone performance, *Filtration and Separation*, 28:188-193.

Hoffmann, A.C., De Groot, M., Peng, W., Dries, H.W.A., Kater, J., 2001, Advantages and risks in increasing cyclone separator length, *AIChE J.*, 47(11):2452-2460.

Knowlton T.M., 2002, A review of catalytic fluidized bed technology reactors in the chemical and petrochemical industrial, in *Proceedings of the IFSA conference, 3-32*, A. Luckos and P. den Hoed (eds), Symposium Series S31, The South African Institute of Mining and Metallurgy.

Muschelknautz, E, 1972,. Die Berechnung von Zyklonabscheidern für Gase (in German), *Chemie-Ing.-Techn.*, 44:63-71.

- Muschelknautz, E., 1980, Theorie der Fliehkraftabscheider mit besonderer Berücksichtigung hoher Temperaturen und Drucke (in German), *VDI-Berichte*, 363:49-60.
- Qiu, K., Yan, J., Li, X., 1999, Experimental study and structure optimization of a uniform square-shaped cyclone separator, *J. Eng. Thermal Energy Power* 14(3).
- Su, Y. Mao, Y., 2006, Experimental study on the gas-solid suspension flow in a square cyclone separator, *Chem. Eng. J.*, 121:51-58.
- Tuzla, K., Chen, J.C., 1992, Performance of a cyclone under high solid loadings, *AIChE Symposium series*, 289:130-136.
- Ushiki, K., Mizuno, M., Sakakibara, H., Utsumi, R., Hata, T., Horiuchi, T., 1993, Experimental study on the performance of very small cyclones for the recycle of ultra-fine powders, *4<sup>th</sup> Int. CFB Conference*:504-510.
- Zenz, F.A., 1999, Cyclone design, in : *Fluidization solids handling and processing industrial applications*, Wen-Ching Yang (eds), Noyes Publ., New Jersey.

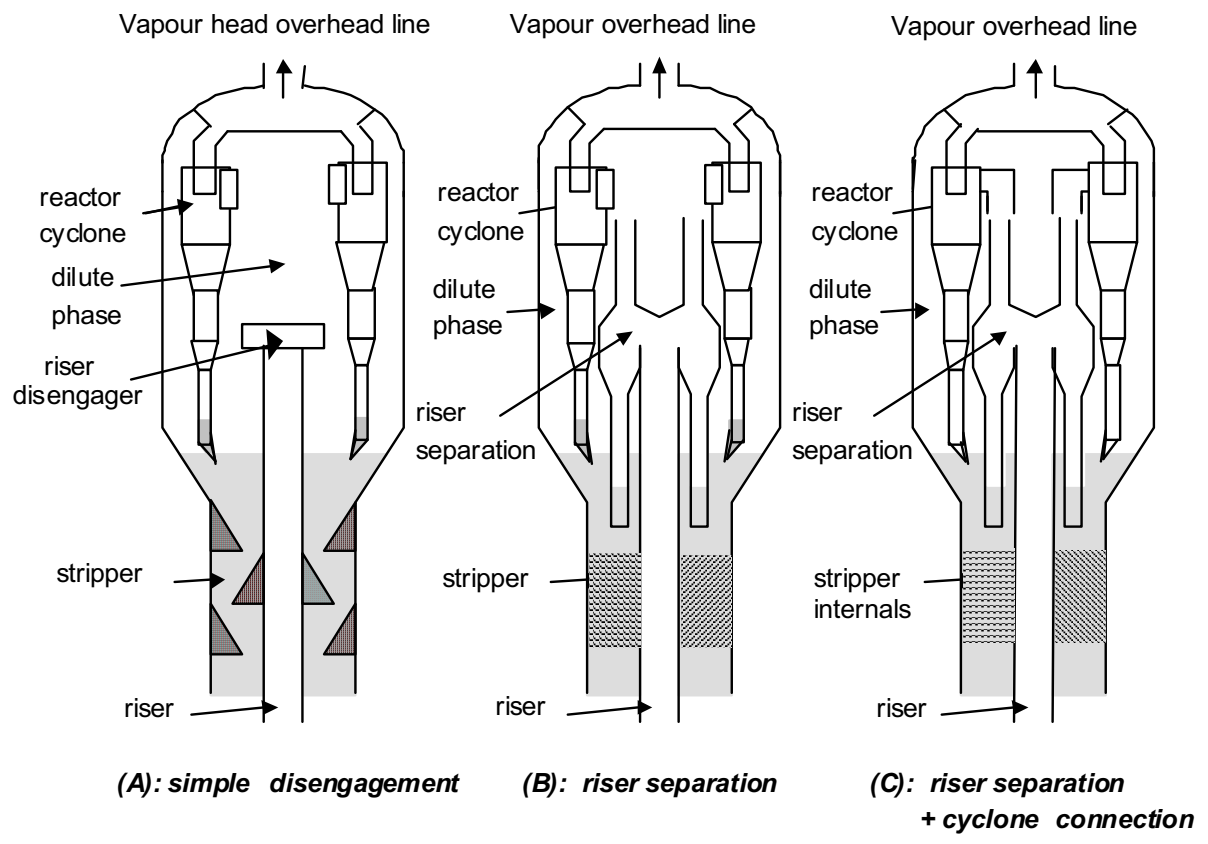


**Figure 1 : Riser termination and reactor design evolution in the FCC process.**

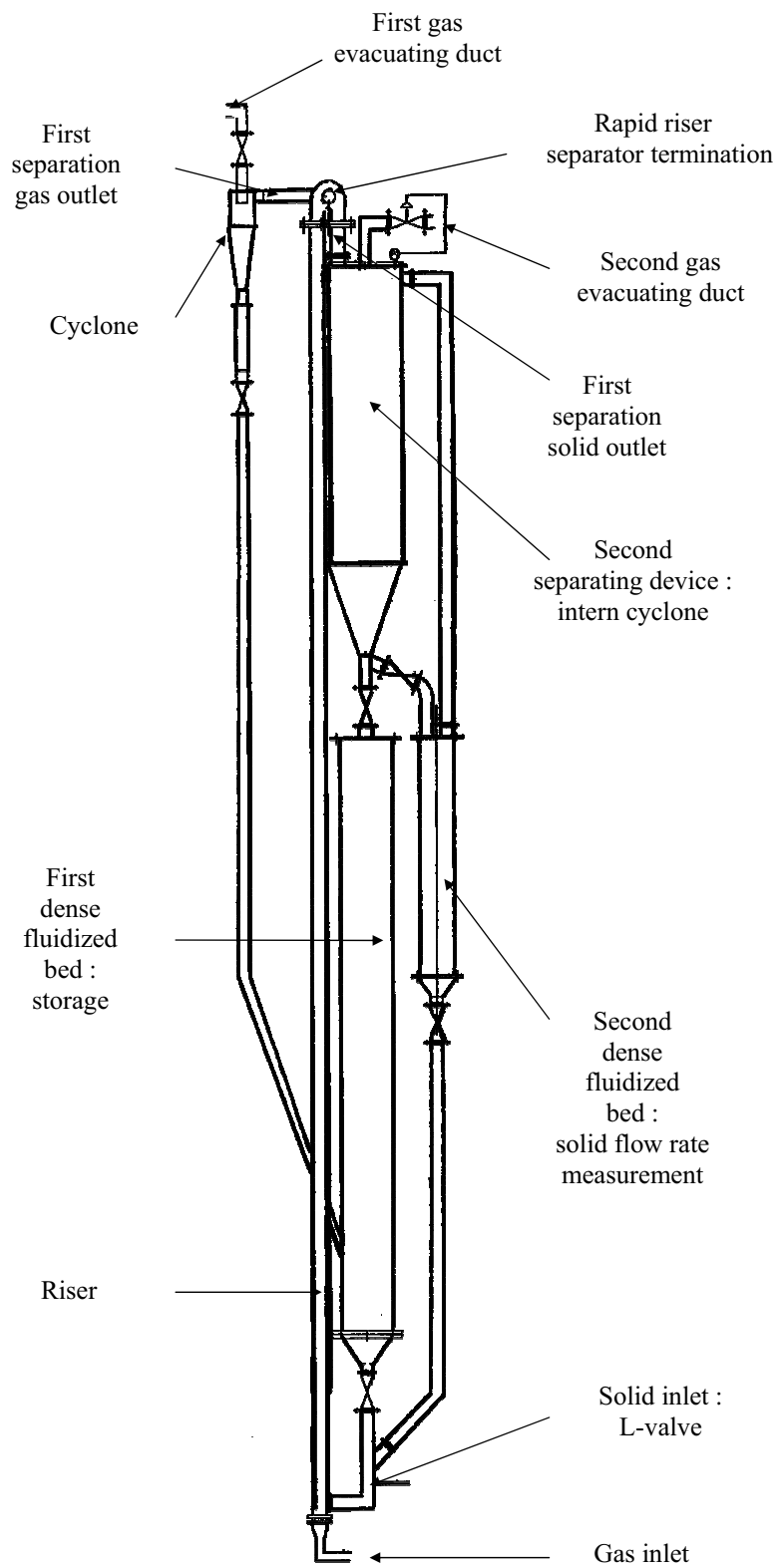


**Figure 2 : The cold pilot**

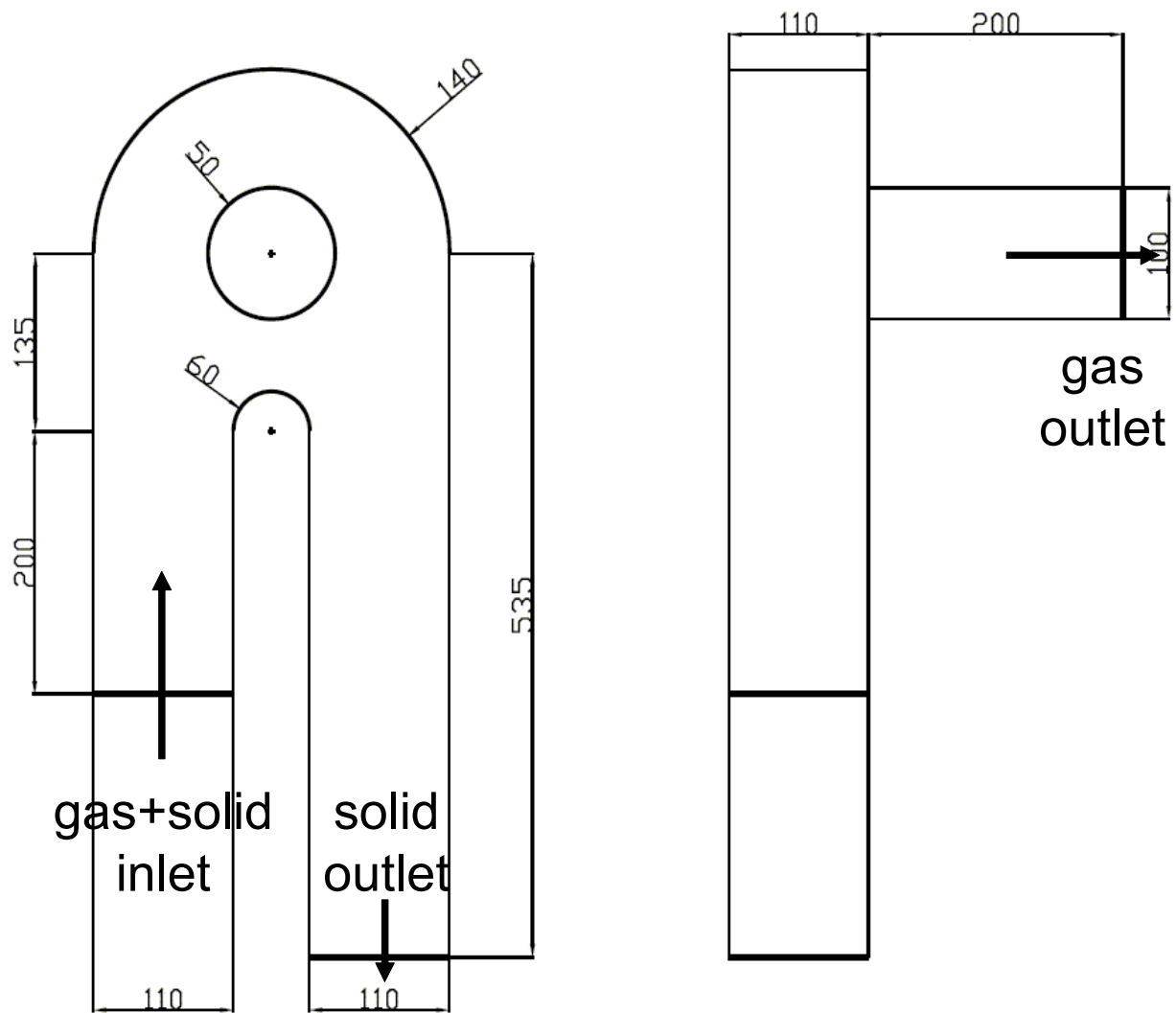


Figure 3 : The separator.



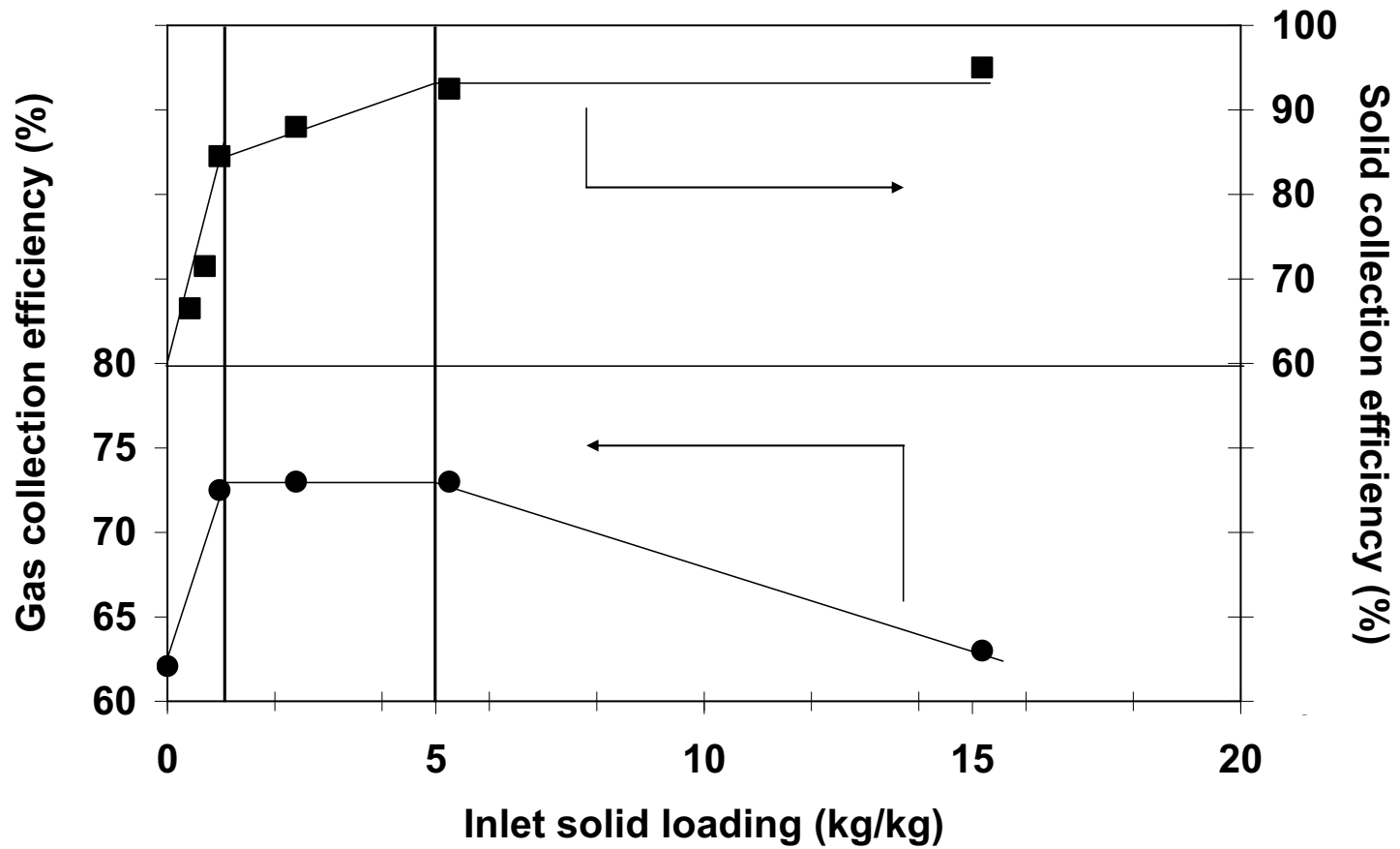


Figure 4 : Gas (●) and solid (■) collection efficiency with no back pressure exerted on the separator dipleg.

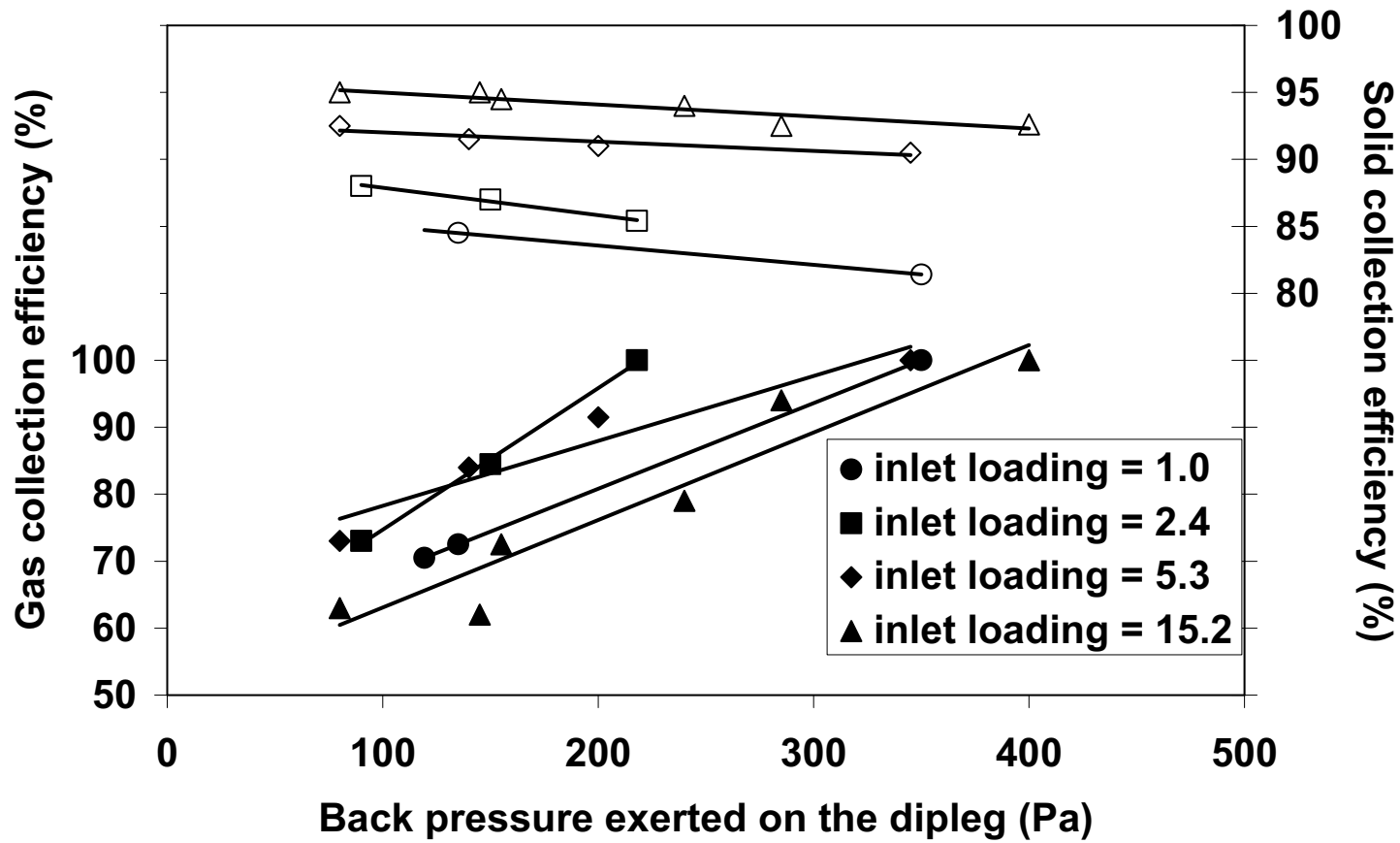


Figure 5 : Effect of the back pressure exerted on gas (filled symbols) and solid (empty symbols) collection efficiencies.

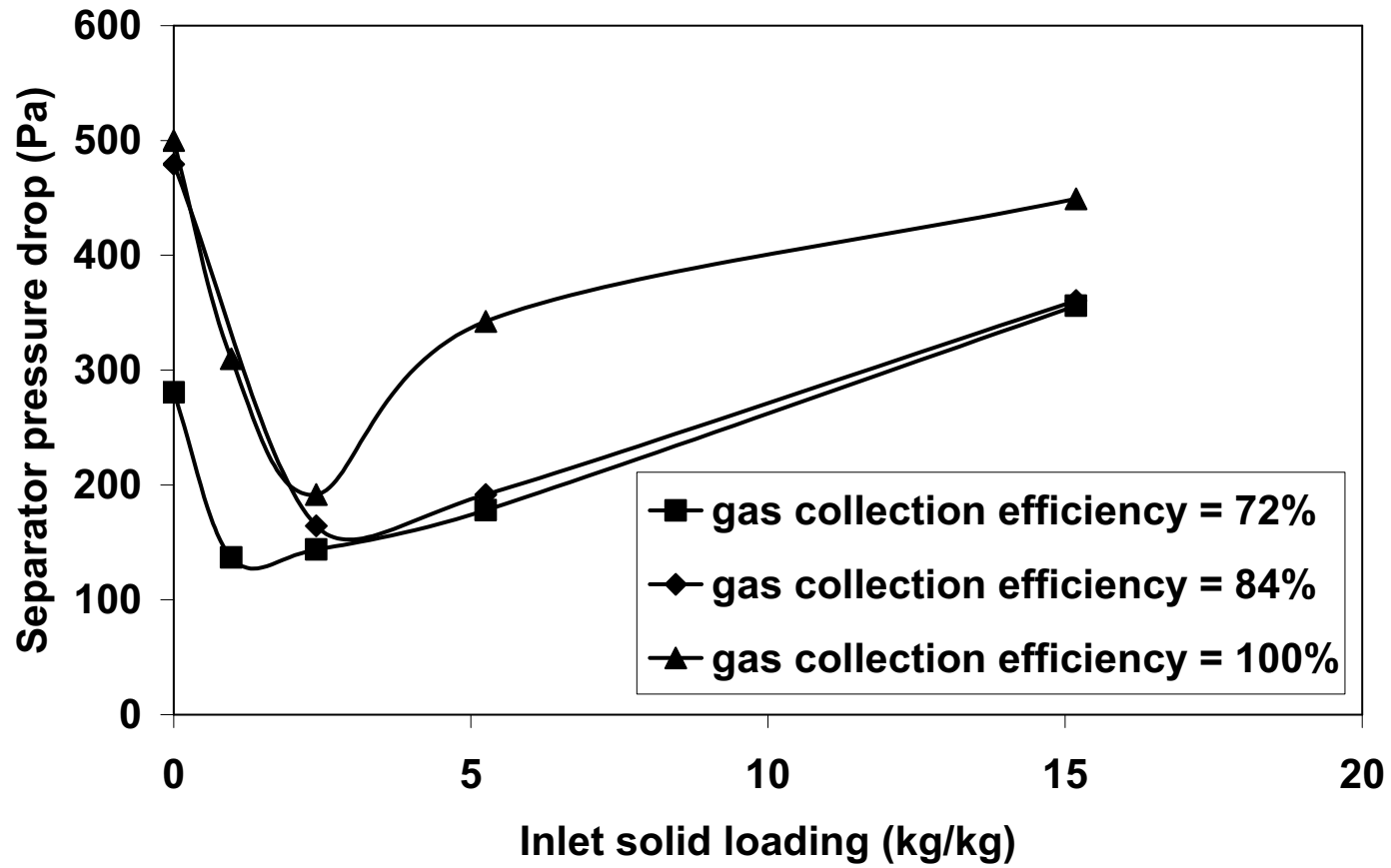


Figure 6 : Effect of the inlet loading on the separator pressure drop between the inlet and the gas outlet at different gas collection efficiency conditions.

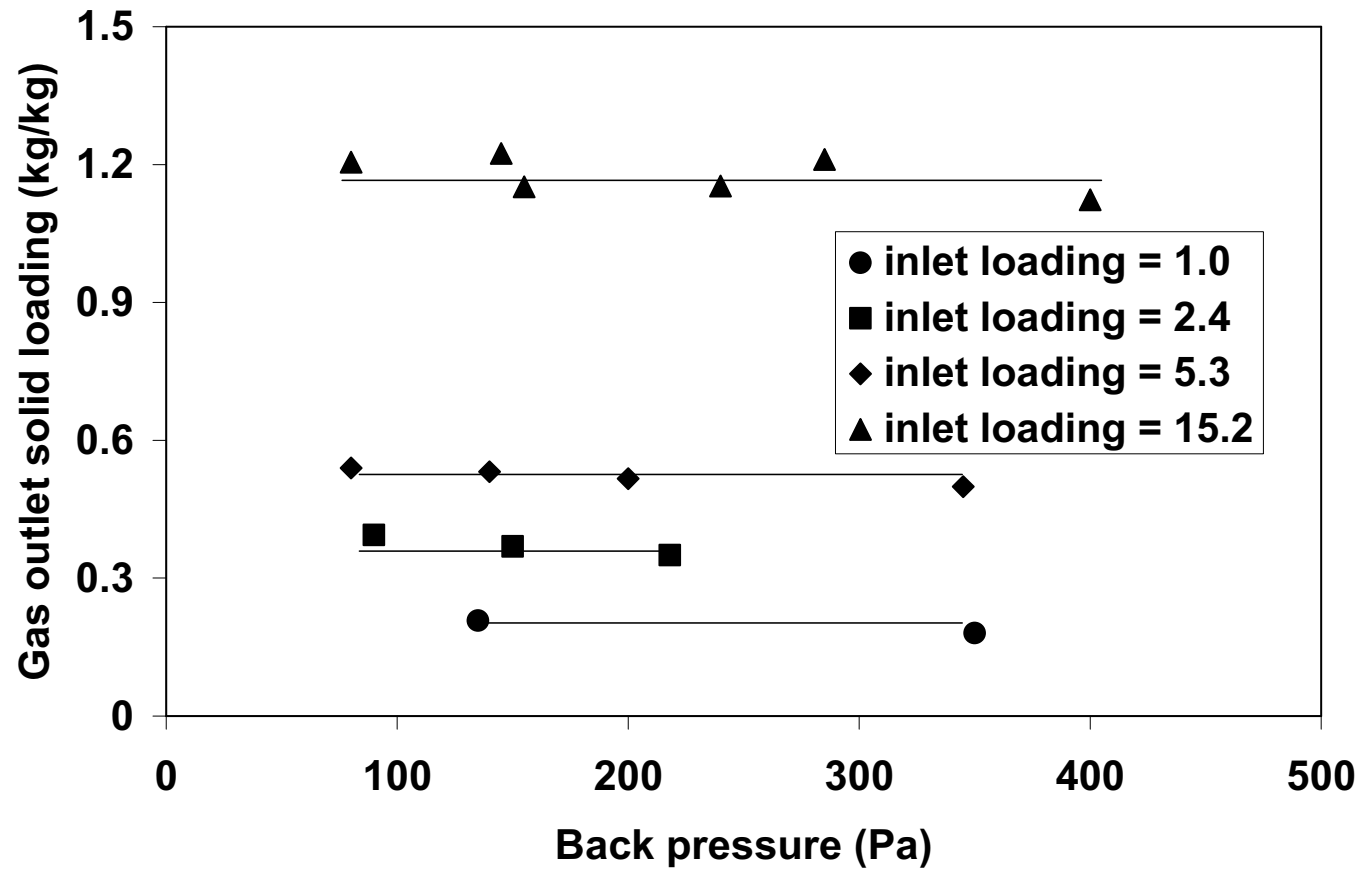
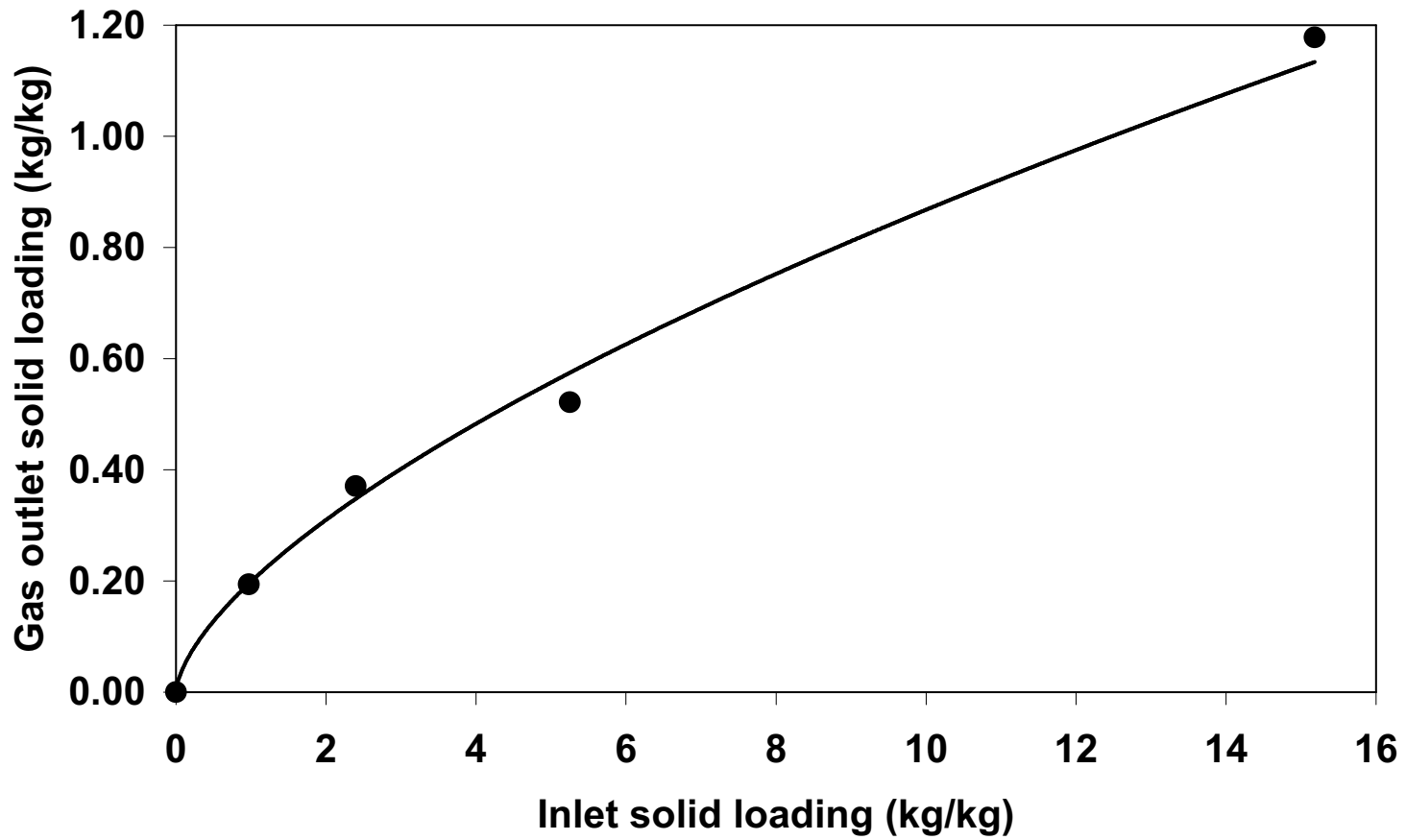


Figure 7 : Gas outlet solid loading for all the studied conditions.



**Figure 8 : Effect of the inlet solid loading on the gas outlet solid loading.**

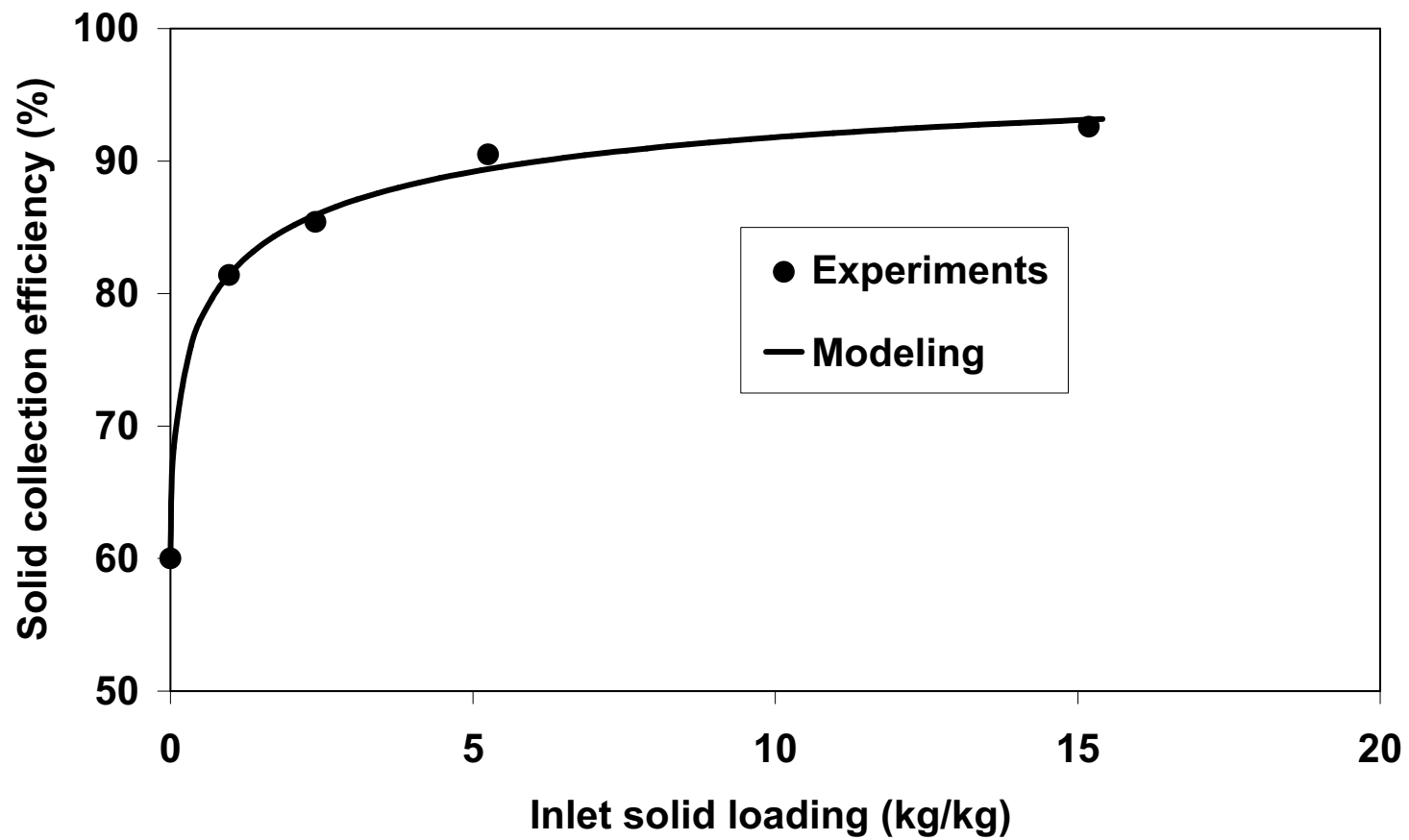


Figure 9 : Solid collection efficiency at 100 % gas collection efficiency. Comparison between experiments and the proposed modeling based on Hoffmann's proposal (1991).

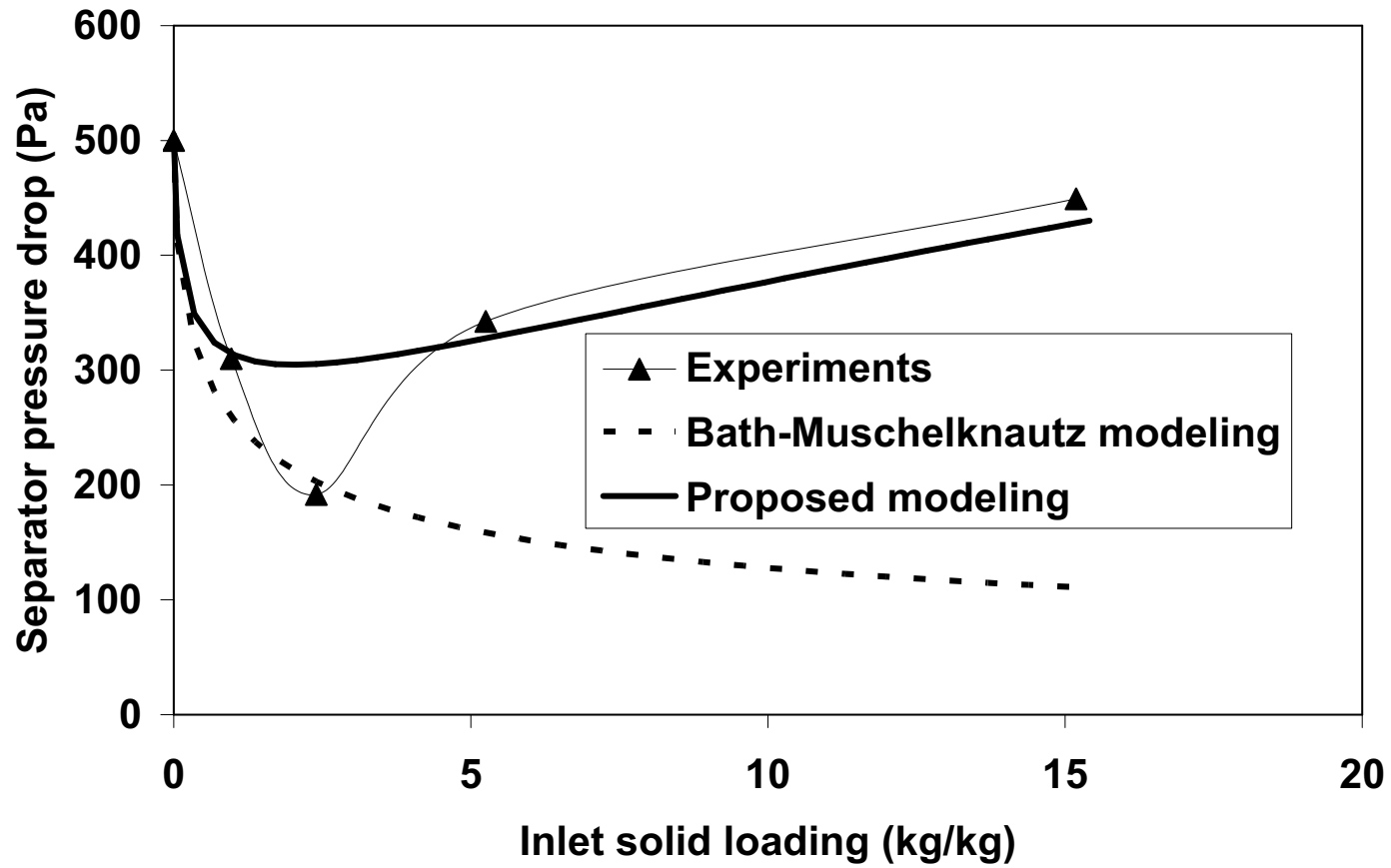


Figure 10 : Comparison between the measured and the predicted pressure drop at 100 % gas collection efficiency. Modeling based on Bath-Muschelknautz.